Hindawi
Journal of Nanomaterials
Volume 2017, Article ID 6092195, 7 pages
https://doi.org/10.1155/2017/6092195

Research Article

TiO_2 Nanotubes with Different Ag Loading to Enhance Visible-Light Photocatalytic Activity

Thi Ngoc Tu Le,[1,2] Nu Quynh Trang Ton,[1] Van Man Tran,[1] Nguyen Dang Nam,[3] and Thi Hanh Thu Vu[1]

[1] *University of Science, 227 Nguyen Van Cu Street, District 5, Ho Chi Minh City, Vietnam*
[2] *Dong Thap University, 783 Pham Huu Lau Street, Ward 6, Cao Lanh City, Dong Thap Province, Vietnam*
[3] *PetroVietnam University, 762 Cach Mang Thang Tam Street, Long Toan Ward, Ba Ria City, Ba Ria-Vung Tau Province, Vietnam*

Correspondence should be addressed to Nguyen Dang Nam; namnd@pvu.edu.vn
and Thi Hanh Thu Vu; vuthihanhthu1979@gmail.com

Received 8 March 2017; Revised 17 May 2017; Accepted 24 May 2017; Published 25 July 2017

Academic Editor: Bo Tan

An improved photocatalytic activity of semiconductor materials using incorporation of the noble metals such as Ag, Au, and Pt is a promising technology. In this study, Ag nanoparticle-TiO_2 nanotube structures (Ag-TNTs) have been investigated as a photocatalyst in different irradiation conditions using different characterization techniques. The results indicate that Ag nanoparticles dispersed uniformly on the TNTs' surface without any change in TNTs' morphology. In addition, Ag-TNTs exhibited lower photoactivity than the TNTs under UV irradiation. In contrast, Ag-TNTs increased the photoactivity in comparison with TNTs and the photocatalytic performance under sunlight irradiation. These phenomena could be contributed to the appearance of Ag nanoparticles on the nanotube surface.

1. Introduction

Various oxide semiconductors have been studied such as ZnO, TiO_2, CdS, WO_3, and SnO_2. TiO_2 has attracted an excellent attention in various applications such as water treatment, air purification, self-cleaning surfaces, antibacterial, and water-splitting catalysts for hydrogen generation [1–3] due to high catalytic efficiency, nontoxicity, being environmentally friendly, wide band gap, and low cost. In recently years, one-dimensional (1D) TiO_2 nanostructures, such as nanorods, nanotubes (TNTs), and nanofiber, have been successfully fabricated and initially effective in environmental treatment [4, 5]. In addition, TNTs remarkably possess superior properties compared with other forms of 1D TiO_2 since TNTs have good mechanical and chemical stability, large surface area, and charge transport property and are highly reproducible [6].

TNTs have been fabricated using different methods such as anodic oxidation, template method, and hydrothermal method [7–9]. Among these technologies, the hydrothermal method may be the best choice due to cost saving, simple processing, and high quality [10]. Unfortunately, a drawback of TiO_2 is its wide band gap (E_g = 3.0–3.2 eV). Therefore, electron-hole pairs generation can only be attained by UV-light irradiation. Moreover, its high recombination rate of photogenerated electron-hole pairs on the surface results in low photocatalytic efficiency. Various strategies have been adopted for improving the photocatalytic efficiency of TiO_2 and extending the absorption spectrum into the visible light region. Making a composite semiconductor by modifying TiO_2 with metal ions is an effective method to extend the light absorption of TiO_2 to the visible light. The transition metal ions act as electron reservoirs to suppress the electron-hole pairs recombination and promote interfacial electron transfer process that increases the surface reactivity. Previous reports have demonstrated that the photocatalytic property of TiO_2 can be improved in combination with transition metal ions, such as Fe, Ni, and Cu, as well as noble metal (Ag, Pt, and Au) [11]. Among these noble metals, Ag is the most suitable for incorporating with TiO_2 to improve

the photocatalytic activity and open possibility for further applications in the antibacterial field due to its strong antimicrobial effect individually. The previous studies have been focused on the photocatalytic properties and the antibacterial ability of Ag nanoparticles loaded TiO_2 under UV light and visible light [12–15]. Nainani et al. [12] reported that Ag-TiO_2 shows higher photocatalytic activity compared to TiO_2 and its absorption and shifting to longer wavelength (visible range) due to lowering of its band gap. Li [13] also reported that the Ag-TiO_2 thin film exhibits higher photocatalytic activity than Degussa P-25 TiO_2 under visible illumination. It is attributed to the deposition of Ag species on the surface layer of TiO_2; an appropriately deposited Ag species on the surface of TiO_2 can effectively capture the photoinduced electrons and holes; besides the photoinduced electrons can quickly be transported to the oxygen adsorbed on the surface of TiO_2. Furthermore, Yi et al. [14] studied Ag/TNT heterojunctions and compared its photocatalytic activity with TNT, P25, and Ag/TNT under visible light due to their extraordinary localized surface plasmon resonance (LSPR) property of Ag nanocrystals and the high adsorption capability of TNTs with the large specific surface area. Gupta et al. [15] compared the antibacterial activity of TiO_2 with Ag-doped TiO_2 nanoparticles on various strains (*Staphylococcus aureus*, *Pseudomonas aeruginosa*, and *Escherichia coli*) under visible light irradiation. Their studies indicated that the enhanced bactericidal activity in the dark and under UV illumination is due to the synergistic antibacterial effect of the photocatalytic reaction of the TiO_2 coating and silver nanoparticles in the matrix. However, these previous works focused on the photocatalytic property of Ag-TiO_2 under UV or visible light irradiation; there are a few reports about the photocatalytic property of Ag-TiO_2 under sunlight condition [16]. Besides that, the average sunshine at 150 kcal/m^2 in Vietnam is between 2.000 and 5.000 hours, which leads to a potential to synthesis application materials in the photocatalytic and antibacterial field. Therefore, in this work, Ag-TiO_2 nanotubes (Ag-TNTs) will be fabricated using the hydrothermal method and photoreduction. The morphology, chemical composition, and crystalline phase of the Ag-TNTs are investigated using various characterization techniques. In addition, the photocatalytic activity of the Ag-TNTs is also evaluated using the absorption of Methylene Blue (MB) aqueous solution at λ = 664.6 nm under UV light and sunlight irradiation conditions. The photocatalyst mechanism is also discussed in detail.

2. Experimental

2.1. Materials Preparation. TNTs were fabricated by the hydrothermal method using 4.2 g of TiO_2 powder dispersed in 120 ml of 10 M NaOH aqueous solution by the magnetic stirrer for 4 hours at 50°C; the TiO_2 + NaOH suspension was then heated at 130°C for 22 hours in an autoclave. After filtration and centrifugation process, the white product was washed with distilled water until pH ~ 9; then 2 M HNO_3 acid was then slowly added to the distilled water until pH 7 and, finally, washed again with not distilled water at 80°C to remove the residue of sodium. Next, this product was dried at 60°C for 4 hours; after that the white powder was annealed in air at 400°C for 2 hours with an increment of 5°C/min.

Ag-TNTs were prepared using the photoreduction method of $AgNO_3$ and TNTs under UV light. Firstly, 0.2 g TNTs were added to 50 ml distilled water and then stirred for 15 min to disperse the TNTs suspension. Different amounts of $AgNO_3$ powder were dissolved in 50 ml distilled water and mixed by the magnetic stirrer at room temperature. Secondly, $AgNO_3$ solution dispersed slowly into the TNTs suspension and was stirred for 15 min to mix in the substances. Thirdly, the solution was stirred for 2 hours under UV irradiation. The Ag-TNTs samples were labeled as Ag-TNTs-2.5, Ag-TNTs-5, and Ag-TNTS-10 based on the concentration of Ag: 2.5 wt.%, 5.0 wt.%, and 10 wt.%, respectively.

2.2. Characterization Techniques. The morphology, crystalline phase, and chemical components of Ag-TNTs were characterized by transmission electron microscopy (TEM, JEM-1400), X-ray diffraction (XRD, Bruker D8-Advance), and AAS (AA-6650, Shimadzu, Japan), respectively. The cyclic voltammetry (CV) and electrochemical impedance spectroscopy (EIS) results were obtained using an electrochemical workstation (Biologic SAS, model 1). A three-electrode system was used for cyclic voltammetry (CV) constituting a counter electrode (platinum mesh), a reference electrode (Ag/AgCl), and a working electrode. The working electrode was prepared by a drop casting method. 5 ml of graphene oxide 0.1 M and 0.05 g TNTs (or Ag-TNTs) solution were dropped on the platinum electrode and allowed to dry out at room temperature. This was repeated until a thin film was formed on top of the platinum electrode, which served as a working electrode. These electrodes were dipped in an electrochemical cell containing 100 ml KCl 0.1 M. Scans were performed between potential ranges of –1 V to 1 V at a scan rate of 10 mVs^{-1} for 100 cycles.

2.3. Photocatalytic Property Tests. The photocatalytic activity of TNTs and Ag-TNTs with a different $AgNO_3/TiO_2$ ratio was investigated by the absorption in an aqueous solution containing MB under different irradiation conditions. 25 mg of each sample was dispersed in 10 ml MB aqueous solution (50 mg/l) and irradiated by UV light (25 W, Reptile UVB100–PT 2187) and sunlight. Every 5 min interval time, TNTs were separated from MB aqueous solution using a centrifuge and filter paper; UV-Vis spectrophotometer (UV-2450; Shimadzu, Tokyo, Japan) was then used for monitoring the absorption of MB solutions at a wavelength of 664.6 nm.

3. Results and Discussions

Figure 1 shows the TNTs and Ag-TNTs with the different $AgNO_3/TiO_2$ ratio. TNTs show the fairly uniform length with a diameter of 11.78 nm with the diameter of Ag-TNTs samples ranging 8–12 nm with the loading of Ag nanoparticles on the tube. It indicated that the appearance of Ag nanoparticles does not affect the morphology of TNTs. At the lowest concentration (2.5 wt.%), there are only a few Ag nanoparticles on the surface of TNTs, when the concentration increases (5.0 wt.%) the density of Ag nanoparticles on

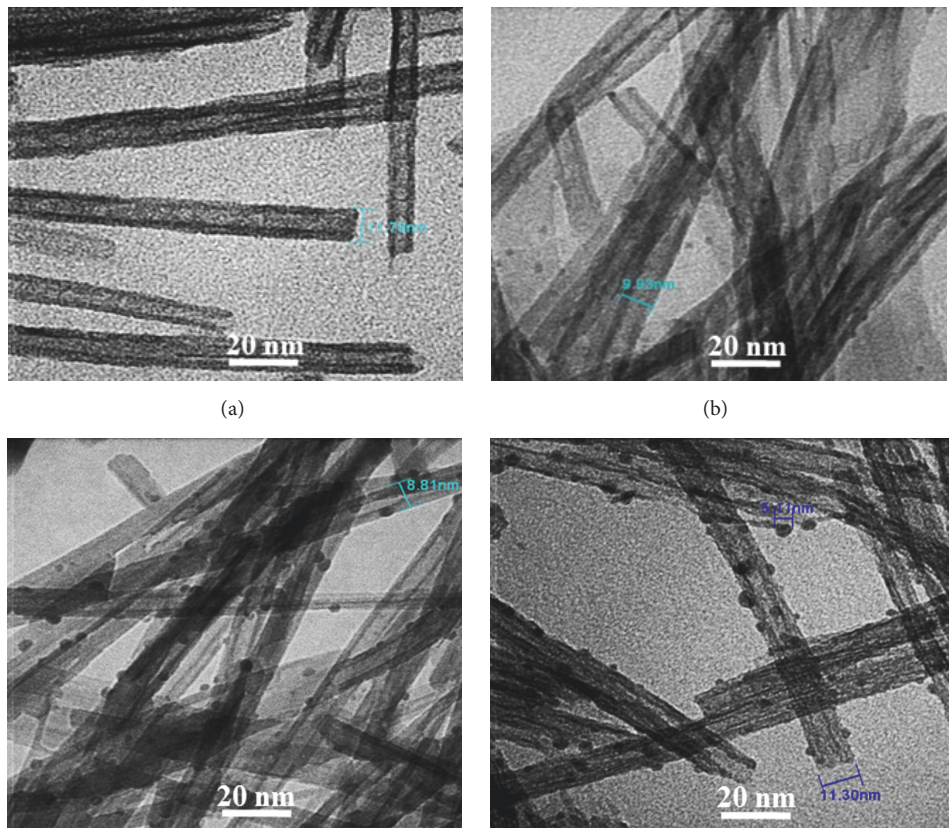

Figure 1: TEM images of (a) TNTs and Ag-TNTs with the different $AgNO_3/TiO_2$ ratio of (b) 2.5, (c) 5.0, and (d) 10.0.

Table 1: AAS result of the Ag concentrations in the Ag-TNTs samples.

Specimens	Ag concentration (μgAg/g sample)
Ag-TNTs-2.5	1172.67
Ag-TNTs-5	2038.67
Ag-TNTs-10	2609.33

TNTs is denser, with the increase nearly covering the TNTs. At the highest concentration (10 wt.%) (Ag-TNTs-10) the size of Ag (Figure 1(d)) is larger than Ag-TNTs-5 sample (Figure 1(c)) and its density is insignificant. These results are fully consistent with the results of AAS analysis in Table 1 and can be explained as follows: the increasing Ag content in samples leads to increasing aggregation phenomena on the surface; in modification process, the filtering and washing possible wash away Ag from TNT-Ag. Therefore, ratio of Ag content after modification process does not agree with ratio of Ag addition.

Figure 2 shows XRD patterns of TNTs, Ag-TNTs-2.5, Ag-TNTs-5, and Ag-TNTs-10. The diffraction peaks appear at 2θ = 25.08°, 27.47°, and 48.05° corresponding to A (101), R (110), and A (200) of TiO_2 anatase, with no other peak species of TiO_2. Besides that, the reflections at 38.04° and 44.8° represented Ag(111) and Ag(200) planes of silver metal. These results indicated that the silver nanoparticles were successfully deposited on the TNTs by the photoreduction method. The deposition process of Ag nanoparticles onto

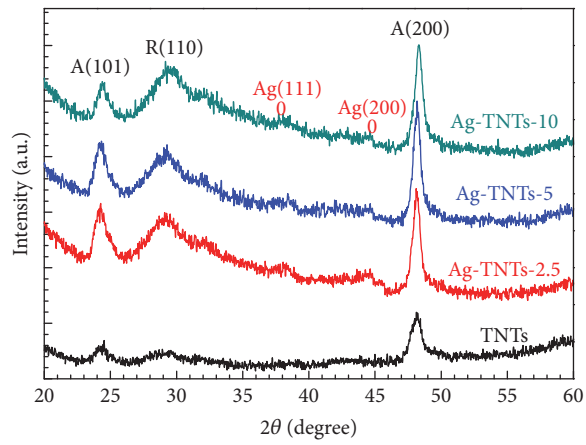

A: anatase
R: rutile

Figure 2: XRD patterns of the TNTs and Ag-TNTs with the different $AgNO_3/TiO_2$ ratio.

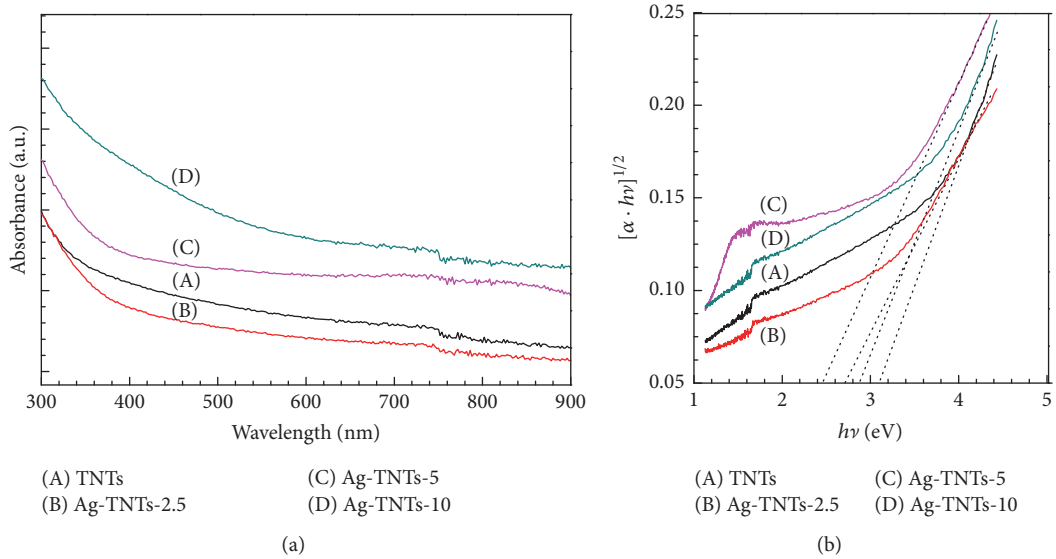

FIGURE 3: UV-Vis absorption spectra of (a) TNTs and Ag-TNTs with different $AgNO_3/TiO_2$ ratio and (b) their plot of $[\alpha h\nu]^{1/2}$ versus photon energy ($h\nu$).

TNTs surface is explained by the mechanism following the reaction equations [17]. First, the TNTs aqueous solution is dispersed in $AgNO_3$ solution, followed by strong magnetic stirring for 2 hours. Silver ions are then adsorbed onto the walls of TNTs due to magnetic stirring under UV irradiation condition. The total deposit of the adsorbed Ag^+ onto the outer surface of TNTs is stronger than onto the inner surface due to the inconvenience of silver ions to travel into smaller areas of inner surface nanotubes:

$$2Ag^+ \longrightarrow 2Ag^+_{\text{absorbed}} \quad (1)$$

$$2Ag^+_{\text{absorbed}} + 2OH^- \longrightarrow 2Ag_2O \downarrow + H_2O \quad (2)$$

The UV irradiation is an extremely important step; TNTs absorb UV radiation and produce electron-hole pairs at the surface of the semiconductor. The photoinduced conduction band electrons are responsible for reducing silver cations into the metallic silver:

$$TiO_2 \xrightarrow{\text{UV}} e^- + h^+ \quad (3)$$

$$Ag_2O + e^- \longrightarrow Ag \quad (4)$$

The UV-vis absorption spectra of TNTs and Ag-TNTs with different $AgNO_3/TiO_2$ ratio are displayed in Figure 3. The absorption spectrum of Ag-TNTs samples shows single broadening at the range of 385.7–504.9 nm, attributing to the charge-transfer from the valence band to the conduction band. The optical band gap energy (E_g) of TNTs and Ag-TNTs was estimated by a plot of $[\alpha h\nu]^{1/2}$ versus photon energy ($h\nu$), using a tangential interception to the x-axis; E_g of TNTs and Ag-TNTs would be calculated by Kubelka-Munk functions and was presented in Figure 3(b). Table 2 shows the wavelength of absorption (λ) and the corresponding band gap (E_g) for TNTs, Ag-TNTs-2.5, Ag-TNTs-5, and Ag-TNTs-10. E_g of Ag-TNTs samples were narrower than that of TNTs,

TABLE 2: Calculated absorption band edge (λ) and band gap (E_g) of TNTs and Ag-TNTs samples.

Specimens	Absorption band edge (λ, nm)	Band gap (E_g, eV)
TNTs	385.7	3.23
Ag-TNTs-2.5	451.7	2.75
Ag-TNTs-5	519.7	2.39
Ag-TNTs-10	504.9	2.46

and the reflectance spectra of Ag-TNTs samples significantly shifted toward a longer wavelength (red shift) compared with TNTs. It proves that the surface modification significantly expanded absorption wavelength region of TNTs due to the surface plasmon resonance of Ag nanoparticles on the surface of TNTs.

The photocatalytic ability of TNTs and Ag-TNTs samples is evaluated by the absorption of MB in the presence of samples under the UV and sunlight irradiation. The absorption peak of MB appeared at 664.6 nm wavelength, and MB absorption efficiency varied with the structural properties of the catalysts. Figure 4(a) shows the absorption spectra of MB solution TNTs and Ag-TNTs with a various $AgNO_3/TiO_2$ ratio under UV irradiation for 30 min. The efficiency of MB absorption is changed corresponding to the structural properties of the catalysts. The absorption spectra for TNTs show the biggest change under UV irradiation condition as shown in Figure 4(a). The degradation efficiency of MB solution of Ag-TNTs-2.5, Ag-TNTs-5, Ag-TNTs-10, and TNTs is about in turn 94.32, 91.46, 90.00, and 99.56, within 45 min (Figure 4(c)), respectively. This result indicated that TNTs show better photocatalytic activity than Ag-TNTs samples under UV irradiation. In contrast, under sunlight condition, Ag-TNTs samples exhibit better photocatalytic activity than TNTs (Figure 4(b)). The degradation efficiency

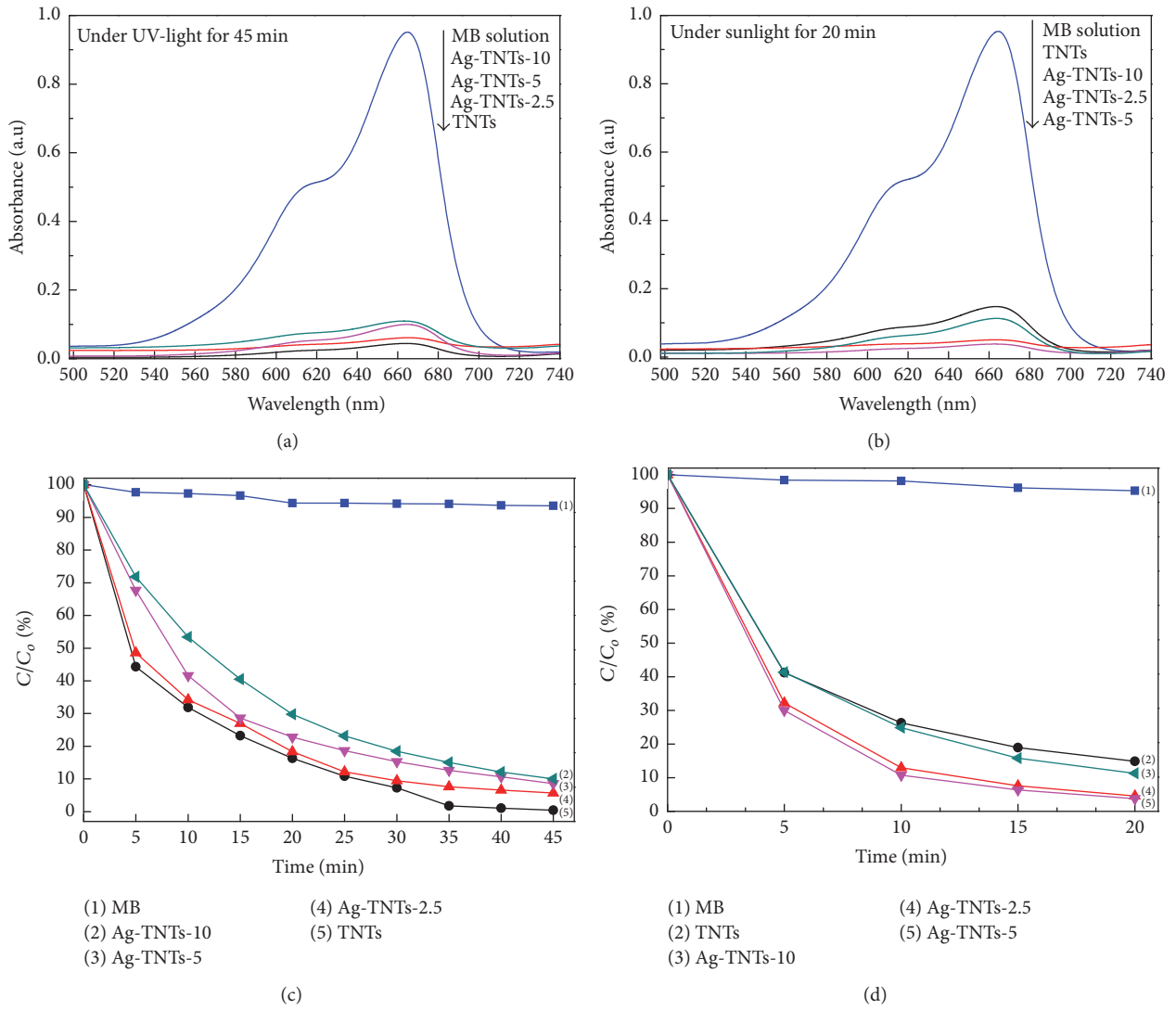

Figure 4: Absorption spectra of MB under (a) UV irradiation and (b) sunlight in the presence of different catalysts. And photocatalytic degradation of MB under (c) UV irradiation and (d) sunlight using various photocatalysts.

of MB solutions in Ag-TNTs-5 is about 96.30 while Ag-TNTs-2.5, Ag-TNTs-10, and TNTs turn in about 95.41, 88.69, and 85.10 within 20 min (Figure 4(d)). It is found that 5.0 wt.% Ag is optimum to achieve the highest degradation efficiency of MB solution under sunlight irradiation. According to the result from Figures 4(a), 4(c), and 4(d), the Ag deposition has the benefits of the photocatalytic activity of all Ag-TNTs samples than TNTs under sunlight irradiation condition. The deposition of Ag nanoparticles on the TNTs surface improved the absorption of MB for the following reasons, and these phenomena were the same as in the previous studies [18, 19]: (i) the formation of Schottky barrier at the Ag nanoparticles-TNTs junction results in Ag nanoparticles deposited on TNTs which have often been applied to act as electron reservoirs to suppress the electron-hole recombination; thus more holes are available for the oxidation reaction, leading to higher photocatalytic activity of TNTs; (ii) more MB molecules are absorbed on the surface of Ag-TNTs than on the TNTs surface, enhancing efficient transfer of the photoexcited electron from MB to the conduction band of TNTs in a self-photosensitization pathway under irradiation; (iii) Ag-TNTs absorb visible light via surface plasmon resonance owing to Ag nanoparticles on the surface TNTs; the plasmon photocatalysis is taking place by injection of electron across the conduction band of TNTs enhancing the surface electron excitation and electron-hole separation. Therefore, the photocatalytic performance of the Ag-TNTs could be better under sunlight condition, whereas Ag nanoparticles deposited on the surface TNTs show the lower photocatalytic activity under UV irradiation condition. It may be explained that the efficiency absorption of MB of Ag-TNTs samples does not significantly contribute to enhancing the TNTs photocatalytic activity under UV; MB molecules are not excited by UV irradiation. Furthermore, the Ag surface plasmon resonance is not excited under UV irradiation.

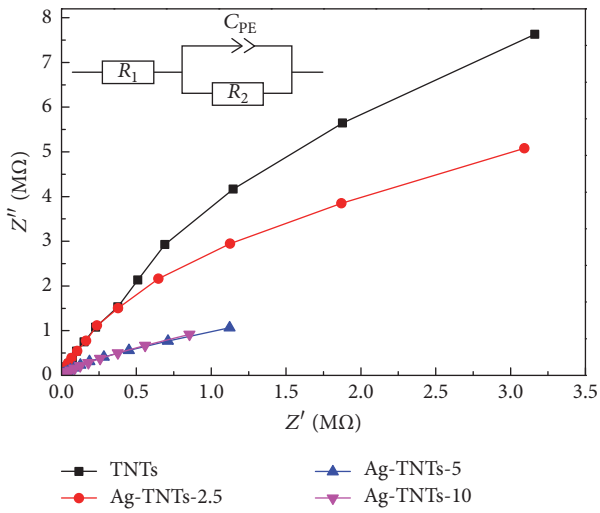

Figure 5: EIS Nyquist spectra of the TNTs and Ag-TNTs with the different $AgNO_3/TiO_2$ ratio.

The Ag content has an important effect on the photocatalytic activity of Ag-TNTs. These results indicated that Ag content of 5.0 wt.% shows the best degradation performance of MB solution under different irradiation. It implies that the photocatalytic activity or the effective electron-hole separation depends on an amount of Ag in TNTs specimens. It could be attributed to the Ag-TNTs surface that acts as electron-hole separation centers, as mentioned in [20]. The electron transfers from the TiO_2 conduction band to metallic Ag nanoparticles at the interface because the Fermi level of TiO_2 is higher than that of Ag metal. It results in the formation of Schottky barrier at metal-semiconductor contact region and improves the photocatalytic activity performance of TiO_2 [21]. However, at an amount of 5.0 wt.% of the silver, that is, a decrease of photocatalytic activity, it can be explained by the following effects [17, 22, 23]: (i) the increasing amount of Ag on the surface of TNTs forms a barrier hindering the contact of MB dye molecules with TNTs [22]; (ii) the Ag nanoparticles prevent the light absorption of TNTs because all of the active sites on the TNTs will be covered by Ag deposition, reducing the efficiency of charge separation increased by the large number of negatively charged Ag particles on the surface TNTs [17, 23]; and (iii) it can also act as the recombination center of electrons and holes, leading to the decrease of photocatalytic activity of TiO_2.

In addition, EIS spectra are used to compare the electronic transportation properties of the TNTs electrode and the Ag-TNTs samples electrode (Figure 5), which is an effective tool for probing the photogenerated charge separation and transport properties [24–26]. The equivalent circuit contains R_1, C_{PE}, and R_2, where R_1 is the bulk resistance of the electrolyte and electrodes and C_{PE} and R_2 are the capacitance and the resistance formed at the interfaces of the electrodes, respectively. The arc radius of Ag-TNTs samples is smaller than TNTs, which shows that the capacitance (C_{PE}) and the resistance (R_2) of Ag-TNTs are larger and smaller than TNTs. A smaller arc radius indicates that the transfer rate and the separation rate of photogenerated electron-hole pairs on the Ag-TNTs arrays' surface become higher due to the appearance of Ag on the surface of TNTs [19]. These results suggest that the photocatalytic Ag-TNTs are higher than TNTs. EIS results are fully consistent with the results of photocatalytic property tests in Figure 4.

4. Conclusions

TNTs were successfully modified with Ag nanoparticles using the photoreduction method. The TNTs have a fairly uniform length of several hundred nanometers and the diameter of about 11.78 nm with Ag nanoparticles decorated on the nanotube surface. Photocatalytic decomposition of MB by Ag-TNTs samples depended on Ag content and irradiation conditions. The TNTs exhibited better photocatalytic activity than Ag-TNTs under the UV irradiation due to the adsorption of dye molecule on the surface of Ag-TNTs and self-degradation of MB. Under sunlight, Ag-TNTs samples showed better photocatalytic activity than TNTs due to the effective electron-hole separation at the interface and the surface plasmon resonance of Ag species. The best photocatalytic performance was obtained when Ag content is 5.0 wt.%. Based on the efficient photocatalytic activity of Ag-TNTs under sunlight, Ag-TNTs have promise for application in the antibacterial field under different light irradiation.

Conflicts of Interest

The authors declare that they have no conflicts of interest.

Acknowledgments

This research is funded by The Science and Technology Department in HCM City in 2016–2018.

References

[1] O. Solcova, L. Spacilova, Y. Maleterova, M. Morozova, M. Ezechias, and Z. Kresinova, "Photocatalytic water treatment on TiO2 thin layers," *Desalination and Water Treatment*, vol. 57, no. 25, pp. 11631–11638, 2016.

[2] Y. Paz, "Application of TiO_2 photocatalysis for air treatment: patents' overview," *Applied Catalysis B: Environmental*, vol. 99, no. 3, pp. 448–460, 2010.

[3] J. Meng, P. Zhang, F. Zhang et al., "A Self-Cleaning TiO_2 Nanosisal-like Coating toward Disposing Nanobiochips of Cancer Detection," *ACS Nano*, vol. 9, no. 9, pp. 9284–9291, 2015.

[4] I. Tamiolakis, I. T. Papadas, K. C. Spyridopoulos, and G. S. Armatas, "Mesoporous assembled structures of Cu," *RSC Advances*, vol. 6, no. 60, pp. 54848–54855, 2016.

[5] C. T. Nam, J. L. Falconer, and W. D. Yang, "Morphology, structure and adsorption of titanate nanotubes prepared using a solvothermal method," *Materials Research Bulletin*, vol. 51, pp. 49–55, 2014.

[6] K. C. Sun, M. B. Qadir, and S. H. Jeong, "Hydrothermal synthesis of TiO2 nanotubes and their application as an overlayer for dye-sensitized solar cells," *RSC Advances*, vol. 4, no. 44, pp. 23223–23230, 2014.

[7] M. P. Neupane, I. S. Park, T. S. Bae, H. K. Yi, F. Watari, and M. H. Lee, "Synthesis and morphology of TiO2 nanotubes by anodic oxidation using surfactant based fluorinated electrolyte," *Journal of the Electrochemical Society*, vol. 158, no. 8, pp. C242–C245, 2011.

[8] K. R. Moonoosawmy, M. Es-Souni, R. Minch, M. Dietze, and M. Es-Souni, "Template-assisted generation of three-dimensionally branched titania nanotubes on a substrate," *CrystEngComm*, vol. 14, no. 2, pp. 474–479, 2012.

[9] N. Roy, Y. Sohn, and D. Pradhan, "Synergy of low-energy and high-energy TiO_2 crystal facets for enhanced photocatalysis," *ACS Nano*, vol. 7, no. 3, pp. 2532–2540, 2013.

[10] N. Liu, X. Chen, J. Zhang, and J. W. Schwank, "A review on TiO_2-based nanotubes synthesized via hydrothermal method: formation mechanism, structure modification, and photocatalytic applications," *Catalysis Today*, vol. 225, pp. 34–51, 2014.

[11] X. Wang, T. Li, R. Yu, H. Yu, and J. Yu, "Highly efficient TiO_2 single-crystal photocatalyst with spatially separated Ag and F^- bi-cocatalysts: orientation transfer of photogenerated charges and their rapid interfacial reaction," *Journal of Materials Chemistry A*, vol. 4, pp. 8682–8689, 2016.

[12] R. Nainani, P. Thakur, and M. Chaskar, "Synthesis of silver doped TiO_2 nanoparticles for the improved photocatalytic degradation of methyl orange," *Journal of Materials Science and Engineering B*, vol. 2, no. 1, pp. 52–58, 2012.

[13] S. Li, "Photoinduced charge property of Ag-TiO_2 films and its relationships with photocatalytic activity under visible illumination," *Surface and Interface Analysis*, vol. 44, no. 7, pp. 851–855, 2012.

[14] J. Yi, S. Zhang, H. Wang, H. Yu, and F. Peng, "Fabrication of uniformly dispersed Ag nanoparticles loaded TiO_2 nanotube arrays for enhancing photoelectrochemical and photocatalytic performances under visible light irradiation," *Materials Research Bulletin*, vol. 60, pp. 130–136, 2014.

[15] K. Gupta, R. P. Singh, A. Pandey, and A. Pandey, "Photocatalytic antibacterial performance of TiO_2 and Ag-doped TiO_2 against *S. aureus.P. aeruginosa* and *E. coli*," *Beilstein Journal of Nanotechnology*, vol. 4, no. 1, pp. 345–351, 2013.

[16] H. M. Sung-Suh, J. R. Choi, H. J. Hah, S. M. Koo, and Y. C. Bae, "Comparison of Ag deposition effects on the photocatalytic activity of nanoparticulate TiO_2 under visible and UV light irradiation," *Journal of Photochemistry and Photobiology A*, vol. 163, pp. 37–44, 2004.

[17] H. Li, X. Duan, G. Liu, and X. Liu, "Photochemical synthesis and characterization of Ag/TiO_2 nanotube composites," *Journal of Materials Science*, vol. 43, no. 5, pp. 1669–1676, 2008.

[18] K. Awazu, M. Fujimaki, C. Rockstuhl et al., "A plasmonic photocatalyst consisting of silver nanoparticles embedded in titanium dioxide," *Journal of the American Chemical Society*, vol. 130, no. 5, pp. 1676–1680, 2008.

[19] X. He, Y. Cai, H. Zhang, and C. Liang, "Photocatalytic degradation of organic pollutants with Ag decorated free-standing TiO_2 nanotube arrays and interface electrochemical response," *Journal of Materials Chemistry*, vol. 21, pp. 475–480, 2011.

[20] W. Zhou, T. Li, J. Wang et al., "Composites of small Ag clusters confined in the channels of well-ordered mesoporous anatase TiO2 and their excellent solar-light-driven photocatalytic performance," *Nano Research*, vol. 7, no. 5, pp. 731–742, 2014.

[21] Q. Lu, Z. Lu, Y. Lu et al., "Photocatalytic synthesis and photovoltaic application of Ag-TiO_2 nanorod composites," *Nano Letters*, vol. 13, no. 11, pp. 5698–5702, 2013.

[22] L. Yang, X. Jiang, W. Ruan et al., "Charge-transfer-induced surface-enhanced raman scattering on Ag-TiO_2 nanocomposites," *Journal of Physical Chemistry C*, vol. 113, no. 36, pp. 16226–16231, 2009.

[23] S. Sakthivel, M. V. Shankar, M. Palanichamy, B. Arabindoo, D. W. Bahnemann, and V. Murugesan, "Enhancement of photocatalytic activity by metal deposition: characterisation and photonic efficiency of Pt, Au and Pd deposited on TiO_2 catalyst," *Water Research*, vol. 38, no. 13, pp. 3001–3008, 2004.

[24] B.-Y. Chang and S.-M. Park, "Electrochemical impedance spectroscopy," *Annual Review of Analytical Chemistry*, vol. 3, no. 1, pp. 207–229, 2010.

[25] W. H. Leng, Z. Zhang, J. Q. Zhang, and C. N. Cao, "Investigation of the kinetics of a TiO2 photoelectrocatalytic reaction involving charge transfer and recombination through surface states by electrochemical impedance spectroscopy," *Journal of Physical Chemistry B*, vol. 109, no. 31, pp. 15008–15023, 2005.

[26] L. Zhao, L. Fang, W. Dong, F. G. Zheng, and M. R. Shen, "Effect of charge compensation on the photoelectrochemical properties of Ho-doped $SrTiO_3$ films," *Applied Physics Letters*, vol. 102, pp. 121905–121909, 2013.